AGU PUBLICATIONS

Paleoceanography

RESEARCH ARTICLE
10.1002/2013PA002552

Key Points:
- Whole-ocean carbon isotope change estimated by benthic foraminiferal d13C
- Mean ocean carbon isotope change of 0.34 ± 0.19 per mil

Supporting Information:
- Readme
- Text S1
- Text S2
- Table S1
- Table S2
- Figure S1
- Figure S2
- Figure S3
- Figure S4
- Figure S5
- Figure S6
- Figure S7

Correspondence to:
C. D. Peterson,
carlye@umail.ucsb.edu

Citation:
Peterson, C. D., L. E. Lisiecki, and J. V. Stern (2014), Deglacial whole-ocean $\delta^{13}C$ change estimated from 480 benthic foraminiferal records, *Paleoceanography*, *29*, 549–563, doi:10.1002/2013PA002552.

Received 16 AUG 2013
Accepted 5 MAY 2014
Accepted article online 9 MAY 2014
Published online 12 JUN 2014

Deglacial whole-ocean $\delta^{13}C$ change estimated from 480 benthic foraminiferal records

Carlye D. Peterson[1], Lorraine E. Lisiecki[1], and Joseph V. Stern[1]

[1]Department of Earth Science, University of California, Santa Barbara, California, USA

Abstract Terrestrial carbon storage is dramatically decreased during glacial periods due to cold temperatures, increased aridity, and the presence of large ice sheets on land. Most of the carbon released by the terrestrial biosphere is stored in the ocean, where the light isotopic signature of terrestrial carbon is observed as a 0.32–0.7‰ depletion in benthic foraminiferal $\delta^{13}C$. The wide range in estimated $\delta^{13}C$ change results from the use of different subsets of benthic $\delta^{13}C$ data and different methods of weighting the mean $\delta^{13}C$ by volume. We present a more precise estimate of glacial-interglacial $\delta^{13}C$ change of marine dissolved inorganic carbon using benthic *Cibicidoides* spp. $\delta^{13}C$ records from 480 core sites (more than 3 times as many sites as previous studies). We divide the ocean into eight regions to generate linear regressions of regional $\delta^{13}C$ versus depth for the Late Holocene (0–6 ka) and Last Glacial Maximum (19–23 ka) and estimate a mean $\delta^{13}C$ decrease of 0.38 ± 0.08‰ (2σ) for 0.5–5 km. Estimating large uncertainty ranges for $\delta^{13}C$ change in the top 0.5 km, below 5 km, and in the Southern Ocean, we calculate a whole-ocean change of 0.34 ± 0.19‰. This implies a terrestrial carbon change that is consistent with recent vegetation model estimates of 330–694 Gt C. Additionally, we find that a well-constrained surface ocean $\delta^{13}C$ change is essential for narrowing the uncertainty range of estimated whole-ocean $\delta^{13}C$ change.

1. Introduction

Dramatic environmental changes during the Last Glacial Maximum (LGM, 19–23 ka) displaced the terrestrial biosphere and decreased the amount of sequestered terrestrial carbon. Because the atmosphere also held less carbon, terrestrial carbon was likely stored in the ocean, the largest carbon reservoir that responds on glacial to interglacial time scales. Previous studies have observed the low isotopic signature of terrestrial carbon ($\delta^{13}C = -25‰$) in the mean benthic $\delta^{13}C$ of the glacial ocean [*Shackleton*, 1977; *Curry et al*., 1988; *Duplessy et al*., 1988]. However, studies based on pollen records, marine records, and modeling have yielded a wide range of estimates for the quantity of terrestrial carbon transferred, from 330 to 1900 gigatons of carbon (Gt C) [*Shackleton*, 1977; *Curry et al*., 1988; *Duplessy et al*., 1988; *Adams and Faure*, 1998; *Crowley*, 1995; *Kaplan et al*., 2002; *Köhler et al*., 2010; *Prentice et al*., 2011; *Ciais et al*., 2011]. Furthermore, previous studies present $\delta^{13}C$ changes for most of the ocean but generally neglect surface water $\delta^{13}C$ change due to the lack of *Cibicidoides* spp. $\delta^{13}C$ data from above 0.5 km. Our study includes estimated changes throughout the ocean with appropriately large uncertainty estimates where direct observations are unavailable, thus giving a whole-ocean estimate appropriate for carbon budget calculations and model-data comparison. Therefore, we generate a revised whole-ocean estimate of marine $\delta^{13}C$ change during the last deglaciation using many more benthic *Cibicidoides* spp. $\delta^{13}C$ measurements than previous studies. These estimates improve our understanding of carbon cycle responses to climate change and, thus, may help constrain estimates of future atmospheric CO_2 change.

2. Background

2.1. Terrestrial Carbon Estimates

The Holocene terrestrial carbon reservoir is estimated to be 2300 Gt C [*Denman et al*., 2007a, 2007b], or up to 3900 Gt C when including inert carbon pools such as soil carbon in permafrost [*Ciais et al*., 2011]. During glacial times, large ice sheets and low temperatures reduce the terrestrial biosphere and displace carbon to the deep-ocean carbon reservoir. The atmosphere, the only other reservoir with a fast enough response time, held 194 Gt C less carbon during glaciations [*Smith et al*., 1999; *Leuenberger et al*., 1992; *Lourantou*, 2008]. However, estimates of glacial-interglacial change in terrestrial biomass (Table 1) vary widely due to differences

Table 1. Deglacial Marine $\delta^{13}C$ and Terrestrial Carbon Storage Change Estimates[a]

Study	Technique	Number of Sites	Carbon Storage Change (Gt C)	$\delta^{13}C$ Change (‰, ±2σ)
Shackleton [1977]	benthic $\delta^{13}C$ (Uvig.)	7	1000[b]	~0.70
Duplessy et al. [1988]	benthic $\delta^{13}C$ (Cibs.)	62	~490[b]	0.32
Curry et al. [1988]	benthic $\delta^{13}C$ (Cibs.)	42	~700[b]	0.46
Boyle [1992]	benthic $\delta^{13}C$ (Cibs.)	65	~490[b]	0.30
Matsumoto and Lynch-Stieglitz [1999]	benthic $\delta^{13}C$ (Cibs.)	124	~468[b]	0.32
Tagliabue [2009]; *Ciais et al.* [2011]	benthic $\delta^{13}C$ (Cibs.)	133	330[c]	0.34 ± 0.26
Crowley [1995]	pollen-based reconstruction	220	750–1050	0.40
Adams and Faure [1998]	paleovegetation reconstruction	29 ecosystems	~1500	—
Köhler et al. [2010]	carbon box model	11 boxes	~500	0.44
Prentice et al. [2011]	DGVM[d]	0.5° grid	550–694	—
This study (0.5–5 km)	benthic $\delta^{13}C$ (Cibs.)	480		0.38 ± 0.08
This study (whole ocean)		480	511 ± 289[b] (330[c])	0.34 ± 0.19

[a]Summary of terrestrial carbon storage decrease estimates from different methods. All uncertainties presented are 95% confidence bounds (2σ). Uvig. = *Uvigerina peregrina*. Cibs. = *Cibicidoides* spp.
[b]The marine $\delta^{13}C$ estimates are converted to carbon storage by equations (1) and (2) which are discussed in section 4.3.
[c]Value calculated using three-reservoir mass balance equations of *Ciais et al.* [2011].
[d]DGVM = dynamic global vegetation model.

in the type and spatial distribution of data analyzed, uncertainties in the distribution of C_3 and C_4 plants, unknown continental shelf and peat land carbon contributions, and model assumptions.

From a 220-site pollen database, *Crowley* [1995] estimated the change in terrestrial carbon storage to be 750–1050 Gt C. This pollen-based estimate has a large uncertainty range due to uncertainties in the distribution of C_3 and C_4 plants during glacials and because of gaps in the distribution of pollen data. The paleovegetation reconstruction of *Adams and Faure* [1998] incorporated a variety of terrestrial paleoenvironmental data including pollen, sedimentary, and paleozoological data. With this diverse paleovegetation data set, *Adams and Faure* [1998] estimated that the total organic carbon storage increased by ~1500 Gt C since the LGM, with a generous uncertainty range (900 to 1900 Gt C) to account for uncertainties in anthropogenic disturbance, bioclimatic zones, no-analog steppe-tundra ecosystem, and peat lands. However, this large of a change had been discounted by several previous studies [*Bird et al.*, 1994, 1996; *Crowley*, 1995].

Using the Box model of the Isotopic Carbon Cycle (BICYCLE) and six control parameters for preindustrial and LGM vegetation and soil carbon contents, the ratio of C_3 and C_4 vegetation, and global net primary productivity, *Köhler et al.* [2010] estimated that mean ocean $\delta^{13}C$ at the LGM was 0.44‰ lower, equivalent to a deglacial change of ~500 Gt C in terrestrial carbon storage. With the sophisticated Land Processes and eXchanges (LPX) dynamic global vegetation (DGV) model, *Prentice et al.* [2011] estimated a global deglacial change in terrestrial carbon storage of 550–694 Gt C.

Ciais et al. [2011] utilized output values of DGV models from the Paleoclimate Modelling Intercomparison Project 2/Models and Observations to Test Climate Feedbacks (MOTIF) database (http://pmip2.lsce.ipsl.fr/) (e.g., LPX) and a variety of proxy data to solve mass balance equations for the mass of terrestrial carbon stored at the LGM and preindustrial. They estimated a terrestrial carbon storage change of 330 Gt C using, in part, a mean ocean deglacial $\delta^{13}C$ change of 0.34 ± 0.26‰ from *Tagliabue et al.* [2009] based on 133 cores with LGM and Holocene data from the MOTIF database (http://motif.lsce.ipsl.fr/). Because the estimated terrestrial carbon change of *Ciais et al.* [2011] is smaller than previous estimates, it implies that ocean carbon storage change may be smaller than previously thought. Our estimate of whole-ocean $\delta^{13}C$ change, based on more sites than *Tagliabue et al.* [2009], is also suitable for use in these mass balance equations.

2.2. Previous Estimates of Global and Regional Marine $\delta^{13}C$ Change

A global marine $\delta^{13}C$ decrease due to changes in the terrestrial carbon reservoir was first proposed by *Shackleton* [1977]. He estimated a change of 0.7‰ based on seven Atlantic and Pacific cores with $\delta^{13}C$ records from *Uvigerina peregrina* and other benthics corrected to *U. peregrina*. However, this species is now known to have a depleted $\delta^{13}C$ signature relative to $\delta^{13}C$ of dissolved inorganic carbon (DIC = ΣCO_2) of

water due to the pore water microhabitat, unlike epibenthic *Cibicidoides wuellerstorfi* which records $\delta^{13}C$ in equilibrium with seawater [*Zahn et al*., 1986]. Carbon isotope measurements based on *C. wuellerstorfi* records are more enriched than measurements from coexisting infaunal species [*Curry et al*., 1988; *Duplessy et al*., 1988].

The estimated change in $\delta^{13}C$ of 0.46‰ from *Curry et al*. [1988] is larger than the estimate of 0.32‰ from *Duplessy et al*. [1988] because *Curry et al*. [1988] only use deep-ocean $\delta^{13}C$ records, whereas *Duplessy et al*. [1988] also include data from intermediate depths (0.7 km in the Pacific, 1 km in the Atlantic). *Curry et al*. [1988] weighted the mean $\delta^{13}C$ of each ocean basin by its volume with a small number of sites in the Indian Ocean ($n = 3$), Southern Ocean ($n = 3$), and Pacific Ocean ($n = 5$), and more sites in the Atlantic Ocean ($n = 32$). In contrast, *Duplessy et al*. [1988] used modern Geochemical Ocean Sections Study (GEOSECS) $\delta^{13}C$ data [*Kroopnick*, 1985] and *Cibicidoides* $\delta^{13}C_{LGM}$ records to estimate the deglacial $\delta^{13}C$ change. To estimate the $\delta^{13}C$ of the shallow high-latitude North Atlantic, they calibrated the planktic *N. pachyderma* $\delta^{13}C$ data according to *Labeyrie and Duplessy* [1985]. Over the entire Atlantic, they used $\delta^{13}C$ water mass geometries to guide interpolation of $\delta^{13}C$ and the water volume of different depth ranges to weight the spatial variations in $\delta^{13}C$ change (Atlantic, $n = 36$). In the Pacific Ocean, however, they used a one-dimensional profile to represent the $\delta^{13}C$ changes with depth and, similarly to the Atlantic, they weighted the $\delta^{13}C$ changes by water volume (Pacific, $n = 26$).

Boyle [1992] and *Matsumoto and Lynch-Stieglitz* [1999] improved on the 1988 estimates with a 1 km resolution volume-weighting technique, and all available *Cibicdoides wuellerstorfi* $\delta^{13}C$ records including numerous new $\delta^{13}C$ records from sparsely sampled regions. The compilation from *Boyle* includes 65 *Cibicidoides* $\delta^{13}C$ records from all three ocean basins (Atlantic, Pacific, and Indian). At each 1 km depth slice, over 1–5 km depth, the mean $\delta^{13}C$ was estimated by eye from $\delta^{13}C$ profiles in six regions: the North Atlantic, Tropical Atlantic, North Pacific, Tropical Pacific, Indian, and Southern Ocean (south of ~45°S). If no glacial $\delta^{13}C$ value was present, *Boyle* used the $\delta^{13}C$ value from the nearest adjacent depth interval. The upper 1 km of the ocean is excluded due to a lack of glacial $\delta^{13}C$ data.

The *Matsumoto and Lynch-Stieglitz* compilation improves spatial coverage with 126 Holocene and 116 LGM $\delta^{13}C$ records spanning 2.5 to 4 km depth in the same six regions as *Boyle* [1992]. They averaged $\delta^{13}C$ measurements in 1 km depth increments from 1 to 5 km depth and then calculated a volume-weighted average. The top 1 km is not included in this "whole-ocean" change. Matsumoto and Lynch-Stieglitz estimate a mean $\delta^{13}C$ change of 0.32‰ and do not estimate the uncertainty of the whole-ocean $\delta^{13}C$. Two simplifications in calculating this whole-ocean estimate include (1) using GEOSECS seawater $\delta^{13}C$ where Holocene benthic $\delta^{13}C$ data are missing and (2) using an assumed deglacial change of 0.32‰ [*Duplessy et al*., 1988] where glacial benthic $\delta^{13}C$ data are missing. Although this second simplification only affects ~10% of their data set, it biases their $\delta^{13}C$ change estimate toward the previously estimated value of 0.32‰ based on fewer observations. In comparison, our study includes benthic $\delta^{13}C$ data from nearly 4 times as many sites, makes locally appropriate extrapolations of $\delta^{13}C$ values where data are missing, and uses a higher-resolution volume weighting.

Oliver et al. [2010] described a 258-core compilation of benthic and planktic foraminiferal $\delta^{13}C$ time series spanning the last 150,000 years. Although they did not estimate a mean carbon isotope shift, they estimated regional mean $\delta^{13}C$ in the deep ocean (below 2.5 km) using a simple (nonvolume-weighted) mean of all $\delta^{13}C$ values in each region. This produced regional $\Delta\delta^{13}C_{Holocene\text{-}LGM}$ estimates of 0.57 ± 0.10‰ in the deep North Atlantic, 0.60 ± 0.18‰ in the deep South Atlantic, and 0.44 ± 0.13‰ in the deep Indo-Pacific. *Hesse et al*. [2011] compiled 220 Atlantic $\delta^{13}C$ records but did not calculate a mean ocean $\delta^{13}C$. *Hesse et al*. [2011] compared their compilation to marine carbon cycle model runs and found the model systematically produced lower than observed $\delta^{13}C$ values. All of the benthic $\delta^{13}C$ records in the *Oliver et al*. [2010] and *Hesse et al*. [2011] compilations are included in our $\delta^{13}C$ compilation.

Tagliabue et al. [2009] estimated a mean $\delta^{13}C$ change of 0.34 ± 0.45‰ using 133 cores with LGM and Holocene data from the MOTIF database (http://motif.lsce.ipsl.fr/). Additionally, the authors calculated an average change of 0.64 ± 0.33‰ for sites below 3 km ($n = 60$). These values represent the arithmetic mean and standard deviation of $\delta^{13}C$ change across all sites, without any volume weighting. However, results from a fully coupled three-dimensional model which reproduces core site $\delta^{13}C$ change with a

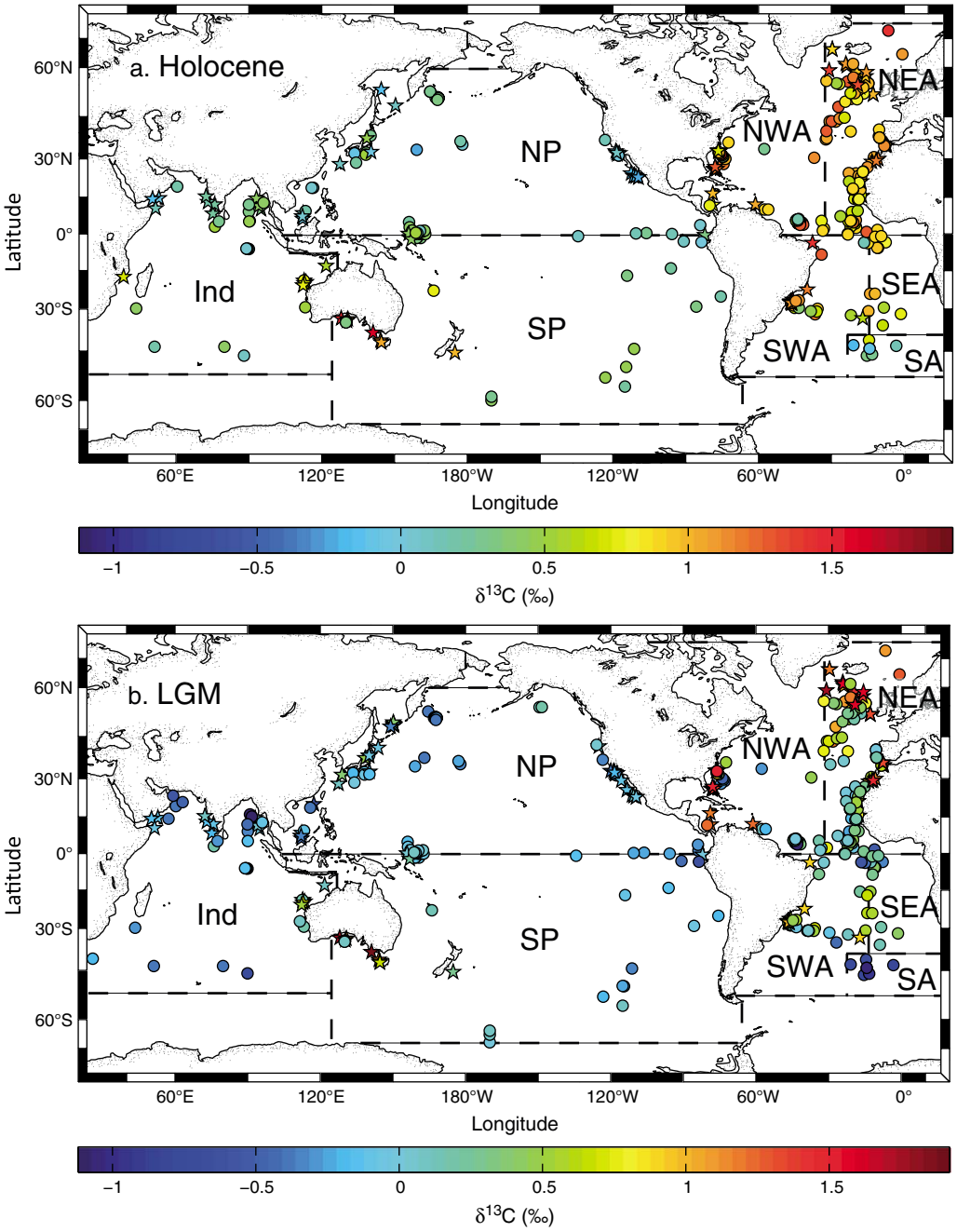

Figure 1. Map of core sites and their (a) Holocene and (b) LGM $\delta^{13}C$ values. Sites shallower than 2 km are plotted as stars, and sites at 2–5 km depth are plotted as circles. Lines demarcate region boundaries (see Table S2 for latitude and longitude of region bounds). Ind = Indian; NP = North Pacific; SP = South Pacific; NWA = Northwest Atlantic; NEA = Northeast Atlantic; SWA = Southwest Atlantic; SEA = Southeast Atlantic; SA = South Atlantic. Complete references for core records are in Table S1.

correlation of 0.6 [*Tagliabue et al.*, 2009] suggested that the sampling error of the mean for these sites compared to the whole ocean is only 0.16‰ [*Ciais et al.*, 2011]. *Ciais et al.* [2011] attributed a total uncertainty range for marine $\delta^{13}C$ change of 0.34 ± 0.26‰ (2σ) using the quadratic sum of instrumental error (0.08‰), proxy error (0.20‰), and sampling error (0.16‰). In contrast, our study estimates whole-ocean $\delta^{13}C$ change by describing the spatial variability of LGM and Holocene $\delta^{13}C$ data from more core locations and without the use of simulated $\delta^{13}C$ estimates, which should provide independent information for model-data comparisons.

Table 2. Number of Cores With $\delta^{13}C$ Data and Ocean Volume[a] for Each Region

Ocean	Region	Holocene Cores	LGM Cores	% Global Volume[a]
Atlantic	NW	61	55	4.9
	NE	110	116	4.3
	SW	44	46	5.0
	SE	37	45	3.5
	S	16	19	0.7
Pacific	N	58	69	21.2
	S	36	38	23.9
Indian		50	50	14.8
Global		412	438	78.3

[a]The percent global volume is the regional volume from 0.5 to 5 km divided by the global volume; our reconstruction over 0.5–5 km constitutes 78.3% of the global ocean volume.

2.3. Ocean $\delta^{13}C$ Spatial Variability

The distribution of carbon in the ocean is spatially complex and changes with time. Spatial variability of $\delta^{13}C$ in the ocean is influenced by fractionation during air-sea CO_2 exchange, photosynthesis, remineralization, and mixing between water masses. Temperature-dependent ocean-atmosphere CO_2 exchange increases the $\delta^{13}C$ of cold surface waters and decreases the $\delta^{13}C$ of warm water [*Zhang et al.*, 1995; *Lynch-Stieglitz et al.*, 1995]. Similarly, photosynthesis enriches the ocean surface in ^{13}C by preferentially removing ^{12}C from the water during the production of organic matter. As ^{13}C-depleted organic matter sinks to the deep ocean, it remineralizes causing $\delta^{13}C$ values at ocean depths below the photic zone to decrease.

Deep overturning circulation affects the spatial distribution of $\delta^{13}C$ by mixing water masses with different $\delta^{13}C$ values. North Atlantic Deep Water (NADW), enriched in ^{13}C, spreads south from the North Atlantic at ~2–4 km. From the Southern Ocean, ^{13}C-depleted Antarctic Intermediate Water (AAIW) flows north into the Atlantic at ~0.5–0.9 km and into the Indian and Pacific Oceans at ~0.5–1.5 km depth. Additionally, ^{13}C-depleted Antarctic Bottom Water (AABW) flows north below ~3 km in the Atlantic [*Johnson*, 2008]. AABW mixes with deeper portions of NADW and flows into the deep Indian and Pacific Oceans where the ^{13}C-depleted water mass is further remineralized. The most ^{13}C-depleted waters occur in the North Pacific where "old" deep water upwells to middepths at ~2 km [*Kroopnick*, 1985; *Matsumoto et al.*, 2002].

During the LGM, deep water formation in the North Atlantic shoaled to above 2 km, which altered water mass mixing ratios and the Atlantic $\delta^{13}C$ distribution [*Curry and Oppo*, 2005]. In the glacial Pacific, ^{13}C-depleted intermediate waters deepened to ~2.5–3 km [*Matsumoto et al.*, 2002]. Some have proposed the existence of an isolated abyssal glacial water mass with light $\delta^{13}C$ values [e.g., *Adkins et al.*, 2002] to explain the "dead carbon" signal present in deglacial atmospheric and surface ocean records [*Hughen et al.*, 1998; *Broecker*, 1998]. However, additional radiocarbon measurements seem to rule out its existence [*Broecker and Clark*, 2010]. Although the global $[CO_3^{2-}]$ changed by ~25–30 μmol kg^{-1} across the deglaciation [*Marchitto et al.*, 2005], this is unlikely to have affected the $\delta^{13}C$ values of *C. wuellerstorfi* because modern $[CO_3^{2-}]$ variations in the Pacific have no effect on the offset between *C. wuellerstorfi* core top $\delta^{13}C$ values and the $\delta^{13}C$ of bottom water DIC [*McCorkle et al.*, 1995]. Therefore, the global decrease in marine $\delta^{13}C$ at the LGM was likely due to terrestrial carbon transfer to the deep ocean as originally proposed by *Shackleton* [1977].

3. Data

To estimate the global ocean mean $\delta^{13}C$ change, we compile published $\delta^{13}C$ measurements for the LGM and Late Holocene of epibenthic foraminifera *Cibicidoides wuellerstorfi* and related genera that preserve the $\delta^{13}C$ of the DIC of the surrounding water [*Woodruff et al.*, 1980; *Zahn et al.*, 1986; *Duplessy et al.*, 1988; *Hodell et al.*, 2001; *Mackensen*, 2008]. Benthic $\delta^{13}C$ data from 480 marine sediment cores were collected from the scientific literature and NOAA, PANGAEA, and Delphi databases (http://www.ncdc.noaa.gov/paleo, http://pangaea.de, http://www.esc.cam.ac.uk/research/research-groups/delphi) (Table S1 in the supporting information). Most of these globally distributed sites have Holocene and LGM time slice $\delta^{13}C$ values, allowing robust reconstructions of both glacial and interglacial climate states. Spatial coverage in the Atlantic and Pacific

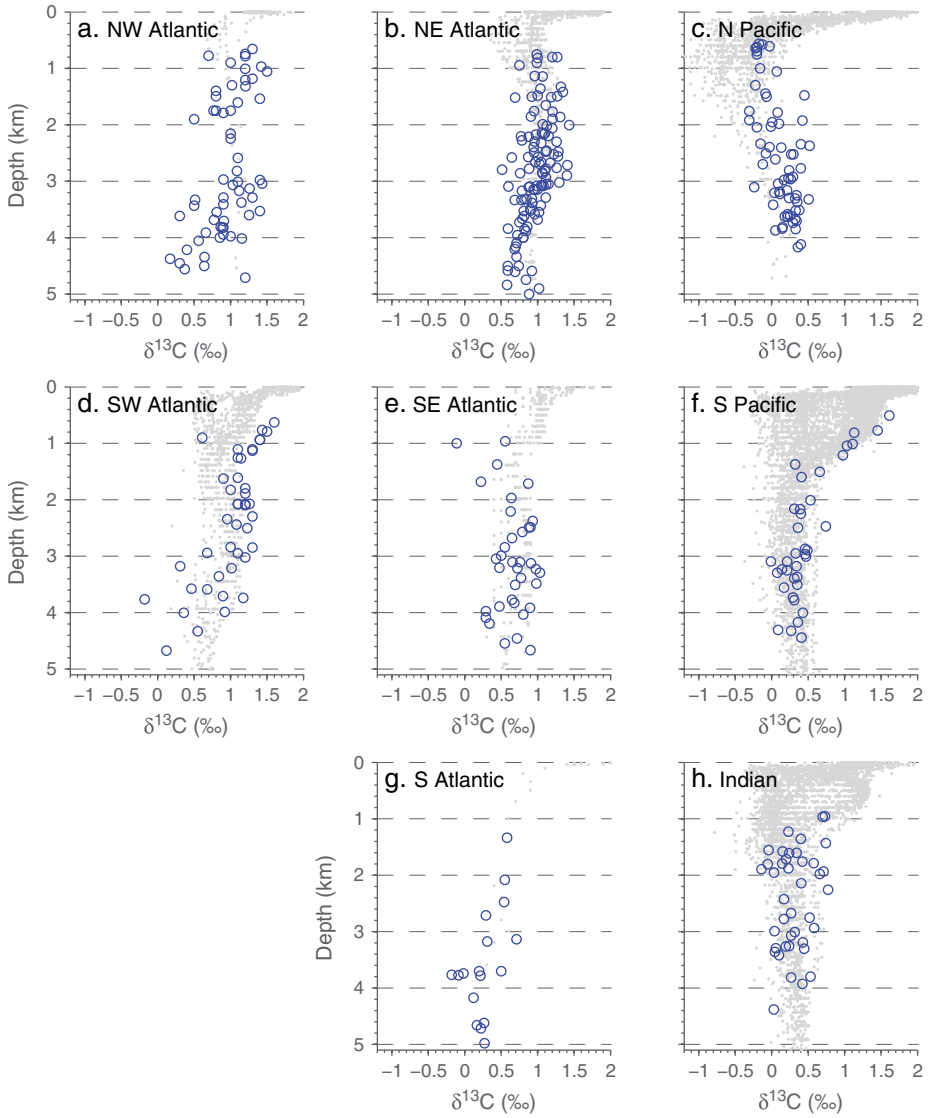

Figure 2. (a–h) Regional Holocene $\delta^{13}C$ data in blue circles and gray modern $\delta^{13}C$ DIC [*Schmittner et al.*, 2013] agree well over the depths the data overlap. A few exceptions discussed in section 6 are the light benthic $\delta^{13}C$ values (relative to modern $\delta^{13}C_{DIC}$) in the SW Atlantic shown in Figure 2d, North and South Pacific shown in Figures 2c and 2f, and the heavy $\delta^{13}C$ values in the deep Western Atlantic (>3 km) shown in Figures 2a and 2d.

Oceans is sufficient to estimate the mean $\delta^{13}C$ separately for different regions in each ocean (Figure 1 and Table 2), which allows us to capture some of the complex variations in $\delta^{13}C$ distributions. Because we compiled a *Cibicidoides*-only data set, sites located in settings with low $\delta^{13}C$ and within the oxygen minimum zone are underrepresented in our estimates. Similarly, *Cibicidoides* records are unavailable from areas of the ocean where carbonate is not preserved or sedimentation rates are very low (e.g., much of the interior of the South Pacific).

Although *Cibicidoides* $\delta^{13}C$ values can be altered in areas of high productivity [*Mackensen et al.*, 1993], comparison between Holocene benthic $\delta^{13}C$ and modern water $\delta^{13}C_{DIC}$ [*Schmittner et al.*, 2013] at nearby locations allows for identification of Holocene benthic $\delta^{13}C$ values that could be subject to the phytodetritus effect [*Mackensen et al.*, 2001] (Figures 2, S1, and S2). Two core sites (MR97-4-3 and MD97-2121) believed to be influenced by the phytodetritus effect by the original authors were excluded from our data compilation. These sites with very low Holocene $\delta^{13}C$ values are located in frontal transition zones and at the confluence of subpolar and subtropical surface currents and hence are sensitive to changes in these regional features

[*Matsumoto et al*., 2002; *Carter et al*., 2008]. The most negative LGM $\delta^{13}C$ values included in our data compilation are −1.12‰ from the NW Atlantic Ocean Drilling Program site 926 [*Lisiecki et al*., 2008] and −1.09‰ at sites MD77-182 and MD77-183 in the Bay of Bengal [*Kallel et al*., 1988]. These Indian sites could be recording weak ventilation in the Northern Indian Ocean during the LGM. However, because there is no Holocene $\delta^{13}C$ data from the Indian cores, it is difficult to determine the cause (e.g., phytodetritus effect) of these low LGM $\delta^{13}C$ values.

4. Methods

4.1. Age Models

We developed new age models for the 141 cores that have both benthic $\delta^{18}O$ and benthic $\delta^{13}C$ time series. These age models are based on $\delta^{18}O$ alignment using Match 2.3 alignment software [*Lisiecki and Lisiecki*, 2002] and regional radiocarbon age models (J. V. Stern and L. E. Lisiecki, manuscript in preparation, 2014), developed using the methodology described in *Stern and Lisiecki* [2013] and detailed in Text S1.

LGM $\delta^{13}C$ values are estimated by averaging all measurements within the age range of 19 to 23 ka. Holocene values are calculated as the average of all measurements within the age range of 0–6 ka because atmospheric CO_2 stabilized by 6 ka [*Sigman and Boyle*, 2000]. Despite this broad definition of the Late Holocene, 75 cores are missing from our Holocene time slice due to loss of surface sediment during coring. We examined the sensitivity of our results to choice of Holocene and LGM time windows and found similar results when these time windows were shifted by as much as 2 kyr. Our compilation also includes 350 $\delta^{13}C$ measurements published in studies that provide LGM and Holocene $\delta^{13}C$ values based on the age models in the original publications (Table S1).

4.2. Regional $\delta^{13}C$ Analysis

We analyze $\delta^{13}C$ data from the Atlantic and Pacific by subdividing these oceans into regions (Figure 1 and Table S2) with distinct water mass characteristics as identified by the depth trends of modern $\delta^{13}C_{DIC}$ and based on the availability of enough data to describe the vertical structure of $\delta^{13}C_{DIC}$ variability (Figures 2, S1, and S2). The Pacific Ocean from 0.5 to 5 km is divided into two regions: the North Pacific, which accounts for 21.2% of global ocean volume, and the South Pacific (23.9% of global ocean volume) (Table 2). One region is used for the Indian Ocean (14.8% volume). The Atlantic Ocean has the largest number of data and is divided into five regions (NW 4.9%, NE 4.3%, SW 5.0%, SE 3.5%, and South 0.7% volume) with distinct water mass characteristics. The east-west boundaries between Atlantic regions are selected to approximately coincide with the changing longitude of the Mid-Atlantic Ridge.

Based on the most southerly locations of cores, the boundary for the portion of the Southern Ocean excluded from our 0.5–5 km calculations is placed at 55°S in the Atlantic and Indian sectors and at 66°S in the Pacific sector. In section 5.2 we address how this excluded portion of the Southern Ocean (6.3% of the global ocean volume) might affect the mean whole-ocean $\delta^{13}C$ change. Sparse data coverage in the Southern Ocean, South Atlantic, and Southeast Atlantic are primarily attributable to poor carbonate preservation. The spatial distribution of Pacific data is limited both by very low productivity and sedimentation rate in some regions and by poor carbonate preservation.

For most regions, one linear regression from 0.5 to 5 km approximates the modern $\delta^{13}C$ depth trend relatively well, given the spatial coverage and noise level of the benthic $\delta^{13}C$ measurements (Figure 3). However, the South Pacific and Indian regions have more complex vertical structures reflecting different water masses and thus require two linear trends to better approximate the depth trends. Additionally, the complex vertical structure in the Southwest Atlantic, resulting from the mixing of AAIW, NADW, and AABW, is approximated with three linear trends. We refrain from using polynomial fits because they are more sensitive to outliers in the data and they are inappropriate for extrapolation [*Runge*, 1901]. The application of linear trends is not meant to imply any particular process associated with benthic $\delta^{13}C$ change. The sensitivity of our mean estimate to the use of linear trends is discussed in more detail in Text S1 (Figures S6 and S7).

Regional linear trends are extrapolated between 0.5 and 5 km for the Holocene and 0.62 and 5.12 km (modern water depth) for the LGM to account for a 120 m decrease in global eustatic sea level [*Fairbanks*, 1989]. We estimated the mean $\delta^{13}C$ every 100 m, weighted the estimate by the regional ocean volume at

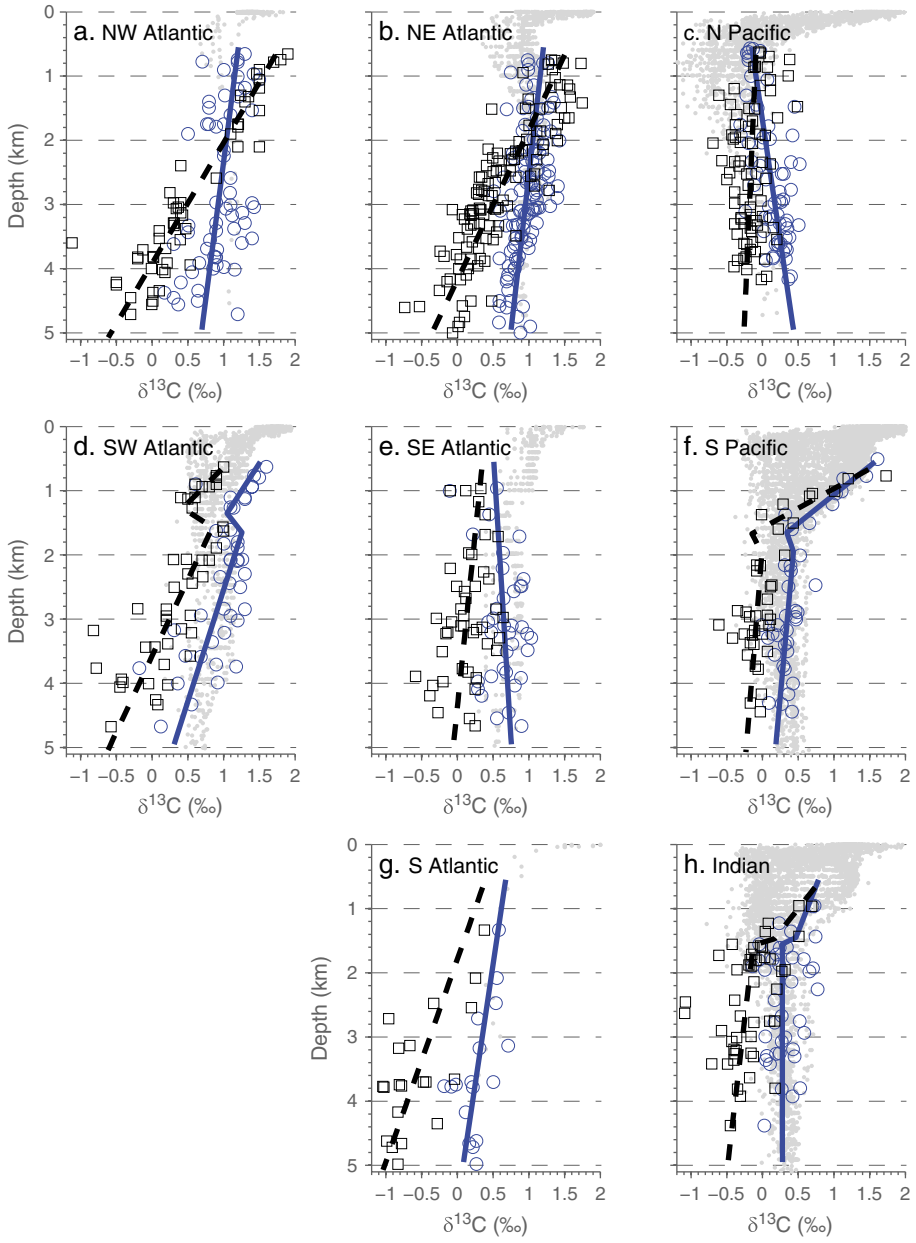

Figure 3. Regional $\delta^{13}C$ data with line fits, gray is modern $\delta^{13}C$ DIC [*Schmittner et al.*, 2013], blue circles are Holocene $\delta^{13}C$ data, and open black squares are LGM $\delta^{13}C$ data.

that depth (±50 m), and then summed over the entire depth range [*Amante and Eakins*, 2009]. For each time slice, all volume-weighted regional $\delta^{13}C$ estimates are summed to produce the global mean $\delta^{13}C$ estimate. Collectively, the volume of this depth range across our eight regions represents 78.3% of the total ocean volume. The Holocene $\delta^{13}C$ estimate is subtracted from the LGM $\delta^{13}C$ estimate for the glacial-interglacial change in mean $\delta^{13}C$ ($\Delta\delta^{13}C_{Hol\text{-}LGM}$).

We evaluated the uncertainty of our estimate using bootstrapping (100,000 iterations) to generate realistic error estimates for the regional line fits of $\delta^{13}C$ versus depth for both the LGM and Holocene time slices. During bootstrapping, we also applied a 2σ uncertainty estimate of 0.15‰ [*Oliver et al.*, 2010] to each data point to account for the internal and external error on each benthic $\delta^{13}C$ measurement. Additionally, we estimate $\delta^{13}C$ uncertainty derived from age model time slice choice to be 0.28‰ (2σ) by assuming ±2 kyr age uncertainty in identification of the Late Holocene and LGM. Age model uncertainty is assumed to be

Table 3. Results of Volume-Weighted Mean $\delta^{13}C$ Estimates (0.5–5 km) for the LGM (19–23 ka) and Holocene (0–6 ka) and the Change in $\delta^{13}C$ With Bootstrapped Uncertainty Estimates

Ocean	Region	Holocene $\delta^{13}C$ (‰)	LGM $\delta^{13}C$ (‰)	$\Delta\delta^{13}C_{Hol\text{-}LGM}$ (‰)	$\pm 2\sigma$ (‰)	Region Volume (% of 0.5–5 km)
Atlantic	NW	0.99	0.75	0.24	0.10	6.3
	NE	1.02	0.76	0.26	0.07	5.5
	SW	0.97	0.35	0.62	0.14	6.4
	SE	0.62	0.17	0.44	0.14	4.4
	South	0.43	−0.22	0.64	0.26	0.8
Total	Atlantic	0.89	0.49	0.41	0.06	23.4
Pacific	North	0.11	−0.17	0.28	0.07	27.1
	South	0.56	0.16	0.39	0.11	30.5
Total	Pacific	0.35	0.01	0.34	0.06	57.6
Indian		0.38	−0.07	0.45	0.36	19.0
Global (0.5–5 km)		0.48	0.11	0.38	0.08	100

independent of internal and external measurement errors, yielding a total 2σ uncertainty of 0.32‰ for each data point. No additional site-specific uncertainties were used because these are not available for most sites. We propagated the bootstrapped linear regressions through all of our calculations to estimate a 95% confidence interval for global $\delta^{13}C$ change and the uncertainty contribution from each region.

4.3. Whole-Ocean and Terrestrial Carbon Change Estimates

To calculate the whole-ocean $\delta^{13}C$ change, in section 5.2 we estimate $\delta^{13}C$ change in the top 500 m (12.7% of global ocean volume), deeper than 5 km (1.9% of global ocean volume), and in the excluded portion of the Southern Ocean (6.3% of the global ocean volume). To assist with comparison to previous studies, we also convert the estimated total mean $\delta^{13}C$ change to terrestrial biomass using equation (1) for our mean $\delta^{13}C_{Hol}$ and $\delta^{13}C_{LGM}$ estimates and equation (2) for studies that publish only mean $\Delta\delta^{13}C_{LGM\text{-}Hol}$:

$$\delta^{13}C_{LGM}(39,000 + M_{TERR}) = -25‰ M_{TERR} + \delta^{13}C_{Hol}(39,000) \quad (1)$$

$$-25‰ M_{TERR} = 39,000\ \Delta\delta^{13}C_{LGM-Hol} \quad (2)$$

where M_{TERR} is the deglacial change in terrestrial carbon storage (Gt C) and the whole-ocean reservoir size is 39,000 Gt C [*Siegenthaler and Sarmiento*, 1993]. We use a mean terrestrial biosphere $\delta^{13}C$ value of −25‰ which is the standard value used in previous studies [*Bird et al.*, 1994; *Crowley*, 1995]. Because this is not the best way to estimate terrestrial biomass change (e.g., due to variability in the $\delta^{13}C$ of vegetation as well as changes in the atmospheric carbon reservoir), this value is provided only for comparison with earlier studies. *Ciais et al.* [2011] present a more comprehensive (and better) technique for calculating terrestrial carbon change which fully accounts for carbon transfer between the three major surface carbon reservoirs (atmosphere, terrestrial biosphere, and ocean) similar to the method in *Bird et al.* [1994]; this is discussed further in section 6.1.

5. Results

5.1. Spatial Variability and Deglacial Change in Benthic $\delta^{13}C$ for 0.5–5 km and $\delta^{13}C$ Trends

The reconstructed pattern of Holocene $\delta^{13}C$ is similar to modern with enriched (more positive) $\delta^{13}C$ values in the North Atlantic and depleted $\delta^{13}C$ values in the Pacific (Table 3). We observe enriched $\delta^{13}C$ values >1‰ at depths shallower than 3 km in the North Atlantic, which is similar to the modern NADW end-member value (1.2‰) [*Broecker et al.*, 1982; *Kroopnick*, 1985] (Figure 4). In the deep South Atlantic, depleted $\delta^{13}C$ values <0.2‰ occur below ~3.5 km depth corresponding to the modern end-member $\delta^{13}C$ of AABW [*Broecker et al.*, 1982]. The most depleted Holocene $\delta^{13}C$ waters occur in the North Pacific at ~2 km depth (−0.36‰) and agree with modern Pacific Deep Water (PDW) end-member $\delta^{13}C$ (<0‰) [*Matsumoto et al.*, 2002]. Similarly, waters corresponding to modern Circumpolar Deep Water (0‰) occur in the South Pacific and Indian Ocean at ~3 km depth.

During the LGM, the most enriched $\delta^{13}C$ values (1.5‰) occur in the Northeast and Northwest Atlantic regions at <1.5 km depth, corresponding to previously estimated values for Glacial North Atlantic

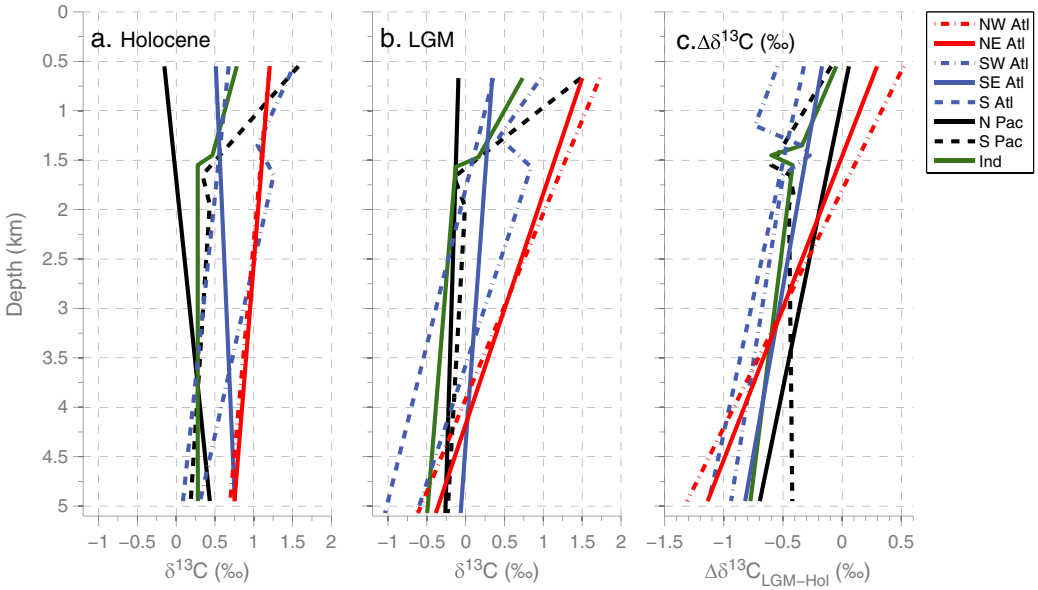

Figure 4. Regional $\delta^{13}C$ line fits from Figure 3 of (a) Holocene, (b) LGM, and (c) LGM-Holocene.

Intermediate Water [*Curry and Oppo*, 2005; *Millo et al*., 2006; *Hesse et al*., 2011]. At 5 km depth we estimate an LGM $\delta^{13}C$ value of −0.5‰ in the Indian Ocean and three Atlantic regions, in approximate agreement with previous AABW estimates [*Ninnemann and Charles*, 2002; *Curry and Oppo*, 2005; *Hesse et al*., 2011]. The deepest South Atlantic and Southwest Atlantic values are estimated at −1‰ and 0‰, respectively, but deep $\delta^{13}C$ data from these regions show particularly large scatter. North and South Pacific LGM $\delta^{13}C$ values are approximately −0.3‰ for nearly all depths below 2 km, with perhaps slightly more negative values near 2 km depth in the North Pacific (Figures 2c and 3c), and deeper than 3 km in the South Pacific (Figures 2f and 3f).

For the depth range of 0.5–5 km, we calculate a mean $\delta^{13}C$ increase of 0.38 ± 0.08‰ from the LGM to the Late Holocene. Overall, the North Atlantic regions have the smallest $\Delta\delta^{13}C_{Hol\text{-}LGM}$ with positive $\delta^{13}C$ shifts at middepths (0.5–2 km) and negative $\delta^{13}C$ change deeper than 2 km (Table 2 and Figure 4). The largest magnitude $\delta^{13}C$ change (>0.6‰) occurs in the Southwest and South Atlantic regions (Figure 4). Most regions show the largest $\delta^{13}C$ change at depths >4 km, but the South Pacific has the largest change at ~2 km (Figures 3f and 4). The largest contributors to uncertainty in our global mean $\delta^{13}C$ estimates for 0.5–5 km are the Indian and South Pacific regions, which have large volumes and relatively sparse data coverage. The availability of records from these locations is scarce because of carbonate dissolution and the habitat range of *Cibicidoides*.

5.2. Whole-Ocean Estimate and Terrestrial Biomass Change

To estimate the deglacial $\delta^{13}C$ change over the whole ocean, we approximate $\delta^{13}C$ changes in the surface ocean (0–500 m depth) and deep ocean (>5 km) using the observed mean change at 500 m and 5 km, respectively (Table 4). Additionally, we assume that the excluded portion of the Southern Ocean $\Delta\delta^{13}C_{0.5\text{–}5\ km}$ (6.3% of the global ocean volume) is identical to the South Atlantic region with larger uncertainty (0.63 ± 0.4‰, 2σ). Because the shape of our Southern Ocean box excludes most of the South Pacific, this estimate primarily represents the Atlantic and Indian sectors of the Southern Ocean. The available modern $\delta^{13}C$ and Holocene $\delta^{13}C$ data from the South Atlantic and South Pacific regions, down to depths of ~3.5 km, agree well with the modern $\delta^{13}C$ and Holocene $\delta^{13}C$ (Figures 2 and S5). The South Atlantic and South Pacific (south of 55°S) may be offset from modern $\delta^{13}C_{DIC}$ by 0.2–0.3‰ due to the phytodetritus effect, although sparse modern $\delta^{13}C$ data in these regions make this relationship difficult to constrain. The inclusion of the Southern Ocean region yields an estimated change of 0.39 ± 0.13‰ for 0.5–5 km depth in the ocean (78.3% of global volume).

The $\delta^{13}C$ change for the top 500 m of the ocean (12.7% of global volume) is difficult to reconstruct due to $\delta^{13}C$ spatial heterogeneity, large uncertainties in geochemical and biological influences on surface ocean $\delta^{13}C$, and

Table 4. Deglacial $\delta^{13}C$ Change Estimates and Percent Volume for Whole-Ocean Estimate Calculation

Whole-Ocean Components	$\Delta\delta^{13}C_{Hol\text{-}LGM}$ ±2σ (‰)	Volume (%)
Surface (0–0.5 km)	0.018 ± 0.40	12.7
0.5–5 km, excluding Southern Ocean Ocean	0.38 ± 0.08	78.3
Southern Ocean (0.5–5 km)	0.63 ± 0.40	6.3
Deep (>5 km)	0.74 ± 0.30	1.9
Whole ocean	0.34 ± 0.19	99.1[a]

[a]Whole-ocean volume does not include high-latitude Arctic, or shallow inland seas.

depth habitat uncertainties among the different planktic foraminifera species. However, 13 globally distributed, but equatorial (20°N–20°S) *Globigerinoides sacculifer* records yield a surface ocean $\delta^{13}C$ of DIC change of 0 ± 0.3‰ [*Broecker and Peng*, 1998]. Additionally, the change in air-sea fractionation would make the deglacial change in the atmospheric $\delta^{13}C$ 0.3‰ more positive than the surface ocean $\delta^{13}C$ of DIC. Compensating for the influence of air-sea fractionation is the Spero effect by which the carbonate ion concentration of the surface waters cause planktic $\delta^{13}C$ to be ~0.3‰ more negative than the surrounding water [*Spero et al.*, 1997]. Combining these factors with the influences of photosynthetic fractionation, sea surface temperature on air-sea fractionation, and changes in deep-ocean circulation, the mean surface ocean $\delta^{13}C$ change falls in the range +0.1–0.3‰ [*Broecker and McGee*, 2013]. To preserve our benthic-only $\delta^{13}C$ estimate, we assume that the mean change for 0–500 m can be approximated using our estimate of global $\delta^{13}C$ change from 500 to 600 m depth, which is 0.018‰, and assign a 2σ uncertainty range of ±0.4‰. Although our surface change estimate (0.018 ± 0.4‰) is smaller than the change estimated by *Broecker and McGee* [2013] (0.1–0.3‰), their estimate lies entirely within our 95% confidence interval. Model-estimated surface changes (0–100 m) of between −0.3‰ and 0‰ [*Köhler et al.*, 2010] fall at the other end of our confidence interval. These widely varying estimates for the top 500 m of the ocean are the largest source of uncertainty in our whole-ocean estimate.

For change in the deep ocean (>5 km), the remaining 1.9% of global volume, we use the observed $\delta^{13}C$ change at 5 km with increased error bars (0.74 ± 0.3‰). Incorporating the estimated global benthic $\delta^{13}C_{0.5–5\ km}$ (0.38 ± 0.08‰), Southern Ocean $\delta^{13}C_{0.5–5\ km}$ (0.63 ± 0.4‰), surface ocean $\delta^{13}C_{0–0.5\ km}$ (0.018 ± 0.4‰), and deep-ocean $\delta^{13}C_{>5\ km}$ changes (0.74 ± 0.3‰), we estimate a whole-ocean mean $\delta^{13}C$ change of 0.34 ± 0.19‰. Using equation (1), this would be equivalent to 511 ± 289 Gt C of terrestrial biomass change.

6. Discussion

6.1. Holocene $\delta^{13}C$ Agreement With Modern Water $\delta^{13}C_{DIC}$

Overall, the Holocene *C. wuellerstorfi* $\delta^{13}C$ data agree well with regional modern $\delta^{13}C$ of DIC over the depths 0.5–5 km (Figure 2); however, some regions of the ocean have very few modern measurements making the relationship difficult to constrain (e.g., South Atlantic). In the SW Atlantic (Figure 2d) and the North and South Pacific (Figures 2c and 2f), the benthic $\delta^{13}C$ values plot on the heavy end of modern $\delta^{13}C_{DIC}$ at intermediate depths (<1.5 km). This may be because benthic $\delta^{13}C$ data are absent in areas of high productivity, low oxygen, and thus low $\delta^{13}C$. In the Western Atlantic (Figures 2a and 2d), some benthic $\delta^{13}C$ values deeper than 3 km are lighter than modern $\delta^{13}C$, possibly as the result of comparing different sample locations for the modern and Holocene data (Figures S1 and S2).

The invasion of anthropogenic CO_2, the Suess effect, causes lighter modern $\delta^{13}C$ values (compared to the Holocene) at depths shallower than 1000 m while nearly 50% of anthropogenic CO_2 is found at depths shallower than 400 m [*Sabine et al.*, 2004]. By comparing Holocene and LGM values, our benthic $\delta^{13}C$ estimates are not influenced by the Suess effect.

Although our foraminiferal calcite $\delta^{13}C$ data may not perfectly capture the full range of $\delta^{13}C_{DIC}$, we can do an excellent job of reconstructing changes in $\delta^{13}C$ at individual sites. Furthermore, our mean change estimate is unchanged if we restrict our calculation to only include sites with both Holocene and LGM $\delta^{13}C$ data ($n = 365$) (Figures S3 and S4). Therefore, within the regions where data are available, our data are well suited for reconstructing $\delta^{13}C$ change. Changes in DIC $\delta^{13}C$ where benthic data $\delta^{13}C$ are not available (e.g., in oxygen minimum zones) are beyond our ability to measure and could potentially bias our results.

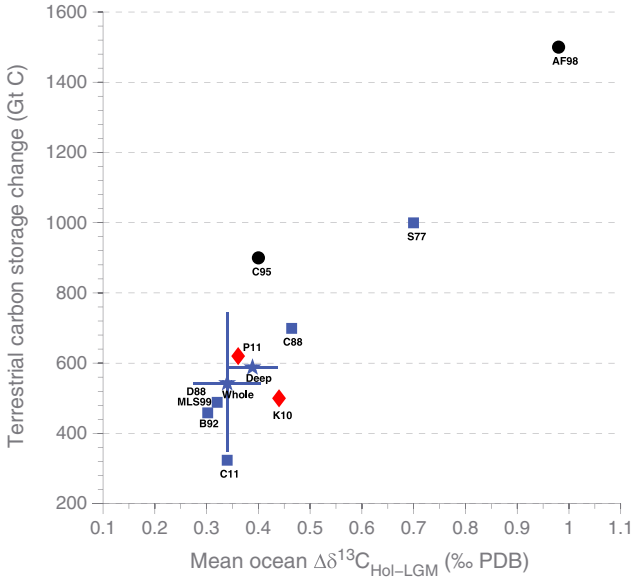

Figure 5. Comparison of our deep-ocean and whole-ocean estimates with previous studies. Marine estimates are denoted by blue squares, our estimates are blue stars; terrestrial carbon storage change estimates for these studies are calculated using equations (1) and (2), as indicated in Table 1. Model-based estimates are red diamonds, and pollen-based and vegetation-based reconstructions are black circles. The error bars on our estimates are 2σ; however, uncertainty estimates from other studies are omitted for clarity. S77 = [*Shackleton*, 1977]; C88 = [*Curry et al*., 1988]; D88 = [*Duplessy et al*., 1988]; B92 = [*Boyle*, 1992]; C95 = [*Crowley*, 1995]; AF98 = [*Adams and Faure*, 1998]; MLS99 = [*Matsumoto and Lynch-Stieglitz*, 1999]; K10 = [*Köhler et al*., 2010]; P11 = [*Prentice et al*., 2011]; C11 = [*Ciais et al*., 2011].

6.2. Comparison With Previous $\delta^{13}C$ Change Estimates

Our estimate of deglacial mean $\delta^{13}C$ change from 0.5 to 5 km (0.38 ± 0.08‰) falls in the middle of previous marine reconstructions of 0.3–0.46‰ (Figure 5). The wide depth range of this study's large data set (480 benthic records) and 100 m resolution volume weightings make our estimate more precise than previous studies. However, a more appropriate "whole-ocean" $\delta^{13}C$ change estimate is 0.34 ± 0.19‰, which represents $\delta^{13}C$ change for 99.1% of the global ocean and accounts for increased uncertainty in $\delta^{13}C$ change outside of the range of benthic $\delta^{13}C$ observations. This value might change slightly if our mean were weighted to account for differing DIC concentrations within the ocean in combination with volume weighting. The largest contribution to uncertainty in the whole-ocean estimates comes from the surface ocean, which accounts for more than 50% of the variance in the whole-ocean uncertainty. This highlights the need for better constraints on surface ocean $\delta^{13}C$ change.

In Figure 6a we compare deep-ocean estimates (1 to 5 km) from the BICYCLE model [*Köhler et al*., 2010] for the Atlantic and Indo-Pacific regions (40°N to 40°S). For this comparison we calculated the mean $\delta^{13}C$ of the deep Atlantic and Indo-Pacific (1 to 5 km) using our regional boundaries excluding the South Atlantic region. The deep Atlantic and deep Indo-Pacific (>1 km) $\delta^{13}C$ estimates from *Köhler et al*. [2010] are more negative than our estimates for both the Holocene and LGM (Figure 6a), and their mean ocean $\Delta\delta^{13}C$ (0.44‰) is larger than our whole-ocean estimate but within 2σ uncertainty (0.34 ± 0.19‰).

Oliver et al. [2010] do not estimate the whole-ocean $\delta^{13}C$ change; however, they do provide regional deep (>2.5 km) mean $\delta^{13}C$ changes that are calculated as the simple mean of all observed values within each region (without accounting for intraregion spatial variability or volume weighting). Our regional estimates for the North Atlantic, South Atlantic, and Indo-Pacific (2.5–5 km) fall within the error bars given by *Oliver et al*. [2010], but we consistently estimate larger changes (Figure 6b). *Oliver et al*. [2010] used data from multiple benthic species and found greater uncertainty in $\delta^{13}C$ changes for species other than *C. wuellerstorfi*. For instance, *McCave et al*. [2008] found that the offset between *U. peregrina* and *C. wuellerstorfi* changes between glacials and interglacials in some locations. Error estimates (2σ) from *Oliver et al*. [2010] include error for the smoothing of $\delta^{13}C$ data, error for cores that are thought to be influenced by the phytodetritus effect, and error for the representativeness of each species for ambient water DIC.

We estimate the same whole-ocean mean $\delta^{13}C$ change (0.34‰) as *Tagliabue et al*. [2009] and *Ciais et al*. [2011] but with a smaller 2σ uncertainty estimate (±0.19‰) than either (±0.45‰ and ±0.26‰, respectively). Our uncertainty is calculated from bootstrapped estimates of $\delta^{13}C$ trends versus depth including a 2σ proxy error estimate of 0.32‰ (for measurement and age model uncertainty) combined with large uncertainties for mean changes in regions without benthic $\delta^{13}C$ data. In contrast, *Ciais et al*. [2011] use 2σ proxy errors of 0.20‰ for differences in sedimentation rates and fractionation effects and 0.08‰ for instrumental uncertainty and combine this with an uncertainty of 0.16‰ due to sample location

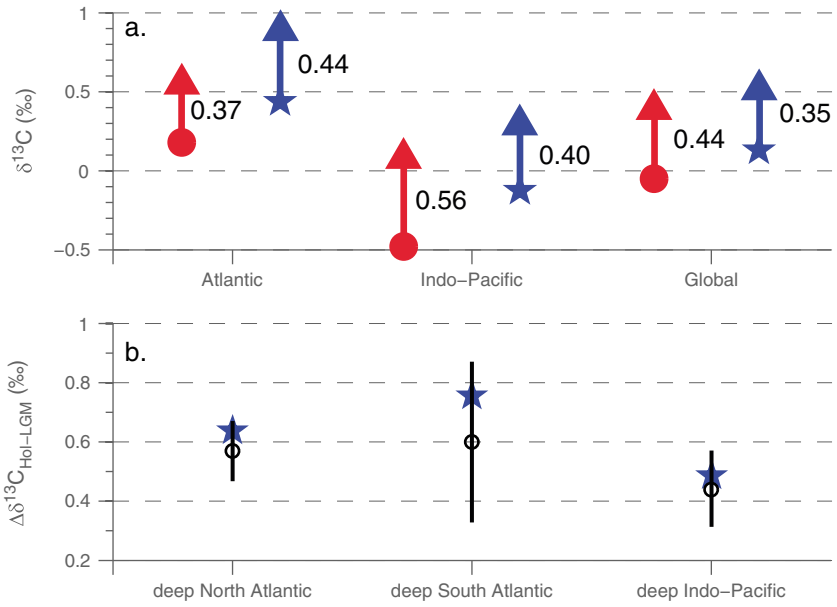

Figure 6. (a) *Köhler et al*. [2010] and (b) *Oliver et al*. [2010] estimates and our estimates (blue stars). The arrows in Figure 6a show the change from the LGM to the Holocene with the numbers indicating the size of the change. Because the regions from the *Köhler et al*. [2010] study are slightly different than ours, we combine our regional δ^{13}C data to estimate over 1–5 km depth for "Atlantic" and "Indo-Pacific" regions to create comparable estimates. Similarly, to compare to *Oliver et al*. [2010] regions, we combine δ^{13}C data from 2.5 to 5 km depth from our regions to estimate deep North Atlantic, deep South Atlantic, and deep Indo-Pacific regions.

bias based on comparison with model-simulated δ^{13}C values. By weighting our δ^{13}C estimates by volume, we eliminate the need to add uncertainty due to sample location bias. Indeed, by estimating spatial variability in benthic δ^{13}C data with more than 3 times as many sites, we demonstrate with less uncertainty and independently of model results that whole-ocean δ^{13}C change was well approximated by *Tagliabue et al*. [2009] and *Ciais et al*. [2011].

Because our global mean δ^{13}C change is the same value used by *Ciais et al*. [2011], our estimate of terrestrial carbon change supports their estimate of 330 Gt C when we use our whole-ocean δ^{13}C change estimate in their mass balance equations. Because this estimate accounts for changes in atmosphere, ocean, and terrestrial carbon, it is the most comprehensive method available for estimating terrestrial carbon change. However, for comparison with previous studies [*Crowley*, 1995; *Broecker and McGee*, 2013], we additionally use equation (1) to convert from marine δ^{13}C change to terrestrial carbon storage change. This method produces an estimate of terrestrial carbon change (511 ± 289 Gt C) which is smaller than pollen- and vegetation-based reconstruction estimates of ~750–1500 Gt C [*Adams and Faure*, 1998; *Crowley*, 1995] but agrees well with recent vegetation model estimates of ~500 Gt C [*Köhler et al*., 2010] and 550–694 Gt C [*Prentice et al*., 2011]. However, the primary result of our study should be considered the mean ocean δ^{13}C change, rather than the estimated terrestrial carbon storage change.

7. Conclusion

We estimate a global marine δ^{13}C change from the LGM to the Late Holocene of 0.38 ± 0.08‰ for 0.5–5 km. This estimate is based on benthic δ^{13}C data from more than 3 times as many locations as previous marine studies [*Curry et al*., 1988; *Duplessy et al*., 1988; *Tagliabue et al*., 2009], uses a more sophisticated volume-weighting technique, and includes bootstrapped uncertainty estimates. Additionally, we estimate a whole-ocean δ^{13}C change of 0.34 ± 0.19‰ using estimated values of 0.018 ± 0.4‰ for the top 500 m of the global ocean, 0.74 ± 0.3‰ for the deep ocean >5 km, and 0.63 ± 0.4‰ for the Southern Ocean. Depending on the conversion technique used, this whole-ocean δ^{13}C change is roughly equivalent to a terrestrial carbon storage change of 330 Gt C or 511 ± 289 Gt C, compatible with recent estimates of 330 Gt C from *Ciais et al*. [2011] and

500–694 Gt C from carbon cycle and vegetation models [*Köhler et al*., 2010; *Prentice et al*., 2011]. Many previous studies which found a similar whole-ocean $\delta^{13}C$ change [*Duplessy et al*., 1988; *Boyle*, 1992; *Matsumoto and Lynch-Stieglitz*, 1999] did so by simultaneously underestimating deep-ocean $\delta^{13}C$ change and excluding the top 1000 m of the ocean. We find that uncertainty in the $\delta^{13}C$ change of the top 500 m of the ocean contributes more than half of the uncertainty in our whole-ocean $\delta^{13}C$ change. Therefore, better constraints for $\delta^{13}C$ changes from 0 to 500 m should be a focus for additional research.

Acknowledgments
We thank G. Gebbie, H. Spero, D. Lea, S. Weldeab, J. Rae, K. Oliver, and one anonymous reviewer for useful suggestions and discussions. Support provided by NSF-MGG 0926735 and NSF-CDI 1125181.

References

Adams, J. M., and H. Faure (1998), A new estimate of changing carbon storage on land since the last glacial maximum, based on global land ecosystem reconstruction, *Global Planet. Change*, *16–17*, 3–24.
Adkins, J. F., K. McIntyre, and D. P. Schrag (2002), The salinity, temperature, and $\delta^{18}O$ of the glacial deep ocean, *Science*, *298*, 1769–1773.
Amante, C., and B. W. Eakins (2009), ETOPO1 1 arc-minute global relief model: Procedures, data sources and analysis, NOAA Technical Memorandum NESDIS NGDC-24, 19.
Bird, M. I., J. Lloyd, and G. Farquhar (1994), Terrestrial carbon storage at the LGM, *Nature*, *371*, 566.
Bird, M. I., A. R. Chivas, and J. Head (1996), A latitudinal gradient in carbon turnover times in forest soils, *Nature*, *381*, 143–146.
Boyle, E. A. (1992), Cadmium and delta 13C paleochemical ocean distributions during the stage 2 Glacial Maximum, *Annu. Rev. Earth Planet. Sci.*, *20*, 245.
Broecker, W. S., T. H. Peng, and Z. Beng (1982), *Tracers in the Sea*, Lamont-Doherty Geological Observatory, Columbia University, Palisades, New York.
Broecker, W. S. (1998), Paleocean circulation during the last deglaciation: A bipolar seesaw?, *Paleoceanography*, *13*(2), 119–121, doi:10.1029/97PA03707.
Broecker, W. S., and T.-H. Peng (1998), *Greenhouse Puzzles*, revised edition Eldigio Press, New York.
Broecker, W., and E. Clark (2010), Search for a glacial-age 14C-depleted ocean reservoir, *Geophys. Res. Lett.*, *37*, L13606, doi:10.1029/2010GL043969.
Broecker, W. S., and D. McGee (2013), The ^{13}C record for atmospheric CO_2: What is it trying to tell us?, *Earth Planet. Sci. Lett.*, *368*, 175–182.
Carter, L., B. Manighetti, G. Ganssen, and L. Northcote (2008), Southwest Pacific modulation of abrupt climate change during the Antarctic Cold Reversal—Younger Dryas, *Palaeogeogr. Palaeoclimatol. Palaeoecol.*, *260*(1), 284–298.
Ciais, P., et al. (2011), Large inert carbon pool in the terrestrial biosphere during the Last Glacial Maximum, *Nat. Geosci.*, *5*, 74–79.
Crowley, T. J. (1995), Ice age terrestrial carbon changes revisited, *Global Biogeochem. Cycles*, *9*, 377–389, doi:10.1029/95GB01107.
Curry, W. B., J.-C. Duplessy, L. Labeyrie, and N. J. Shackleton (1988), Changes in the distribution of d ^{13}C of deep water ΣCO_2 between the last glaciation and the Holocene, *Paleoceanography*, *3*, 317–341, doi:10.1029/PA003i003p00317.
Curry, W. B., and D. W. Oppo (2005), Glacial water mass geometry and the distribution of δ13C of ΣCO2 in the western Atlantic Ocean, *Paleoceanography*, *20*, PA1017, doi:10.1029/2004PA001021.
Denman, K. L., et al. (2007a), Couplings between changes in the climate system and biogeochemistry, in *IPCC Climate Change 2007: The Physical Science Basis*, edited by S. Solomon et al., chap. 7, pp. 499–587, Cambridge Univ. Press, New York.
Denman, K. L., et al. (2007b), Couplings between changes in the climate system and biogeochemistry, in *Climate Change 2007: The Physical Science Basis. Contribution of Working Group I to the Fourth Assessment Report of the Intergovernmental Panel on Climate Change*, edited by S. Solomon et al., pp. 499–588, Cambridge Univ., Cambridge.
Duplessy, J. C., N. J. Shackleton, R. G. Fairbanks, L. Labeyrie, D. Oppo, and N. Kallel (1988), Deepwater source variations during the last climatic cycle and their impact on the global deepwater circulation, *Paleoceanography*, *3*, 343–360, doi:10.1029/PA003i003p00343.
Fairbanks, R. G. (1989), A 17,000-year glacio-eustatic sea-level record: Influence of glacial melting rates on the Younger Dryas event and deep ocean circulation, *Nature*, *342*, 637–642, doi:10.1038/342637a0.
Hesse, T., M. Butzin, T. Bickert, and G. Lohmann (2011), A model-data comparison of $\delta^{13}C$ in the glacial Atlantic Ocean, *Paleoceanography*, *26*, PA3220, doi:10.1029/2010PA002085.
Hodell, D. A., S. L. Kanfoush, A. Shemesh, X. Crosta, C. D. Charles, and T. P. Guilderson (2001), Abrupt cooling of Antarctic surface waters and sea ice expansion in the South Atlantic sector of the Southern Ocean at 5000 cal yr B.P, *Quat. Res.*, *56*(2), 191–198.
Hughen, K. A., J. T. Overpeck, S. J. Lehman, M. Kashgarian, J. Southon, L. C. Peterson, R. Alley, and D. M. Sigman (1998), Deglacial changes in ocean circulation form an extended radiocarbon calibration, *Nature*, *391*, 65–68.
Johnson, G. C. (2008), Quantifying Antarctic bottom water and North Atlantic deep water volumes, *J. Geophys. Res.*, *113*, C05027, doi:10.1029/2007JC004477.
Kallel, N., L. D. Labeyrie, A. Juillet-Leclerc, and J. C. Duplessy (1988), A deep hydrological front between intermediate and deep-water, masses in the glacial Indian Ocean, *Nature*, *333*, 651–655.
Kaplan, J. O., I. C. Prentice, W. Knorr, and P. J. Valdes (2002), Modeling the dynamics of terrestrial carbon storage since the Last Glacial Maximum, *Geophys. Res. Lett.*, *29*(22), 2074, doi:10.1029/2002GL015230.
Köhler, P., H. Fischer, and J. Schmitt (2010), Atmospheric $\delta^{13}CO_2$ and its relation to pCO_2 and deep ocean $\delta^{13}C$ during the late Pleistocene, *Paleoceanography*, *25*, PA1213, doi:10.1029/2008PA001703.
Kroopnick, P. (1985), The distribution of 13C of TCO_2 in the world oceans, *Deep Sea Res.*, *32*, 57–84.
Labeyrie, L. D., and J. C. Duplessy (1985), Changes in the oceanic 13C/12C ratio during the last 140 000 years: High-latitude surface water records, *Palaeogeogr. Palaeoclimatol. Palaeoecol.*, *50*, 217–240.
Leuenberger, M., U. Siegenthaler, and C. C. Langway (1992), Carbon isotope composition of atmospheric CO_2 during the last ice age from an Antarctic ice core, *Nature*, *357*(6378), 488–490.
Lisiecki, L. E., and P. A. Lisiecki (2002), Application of dynamic programming to the correlation of paleoclimate records, *Paleoceanography*, *17*(4), 1049, doi:10.1029/2001PA000733.
Lisiecki, L. E., M. E. Raymo, and W. B. Curry (2008), Atlantic overturning responses to Late Pleistocene climate forcings, *Nature*, *456*, 85–88.
Lourantou, A. (2008), Constraints on the carbon dioxide (CO_2) deglacial rise based on its stable carbon isotopic ratio ($\delta^{13}CO_2$), PhD thesis, 214 pp., Université Joseph Fourier.
Lynch-Stieglitz, J., T. F. Stocker, W. S. Broecker, and R. G. Fairbanks (1995), The influence of air-sea exchange on the isotopic composition of oceanic carbon: Observations and modeling, *Global Biogeochem. Cycles*, *9*, 653–665, doi:10.1029/95GB02574.

Mackensen, A. (2008), On the use of benthic foraminiferal $\delta^{13}C$ in palaeoceanography: Constraints from primary proxy relationships, *Geol. Soc. Lond. Spec. Publ.*, *303*, 121–133.

Mackensen, A., H. W. Hubberten, T. Bickert, G. Fischer, and D. K. Fütterer (1993), The $\delta^{13}C$ in benthic foraminiferal tests of Fontbotia wuellerstorfi (Schwager) relative to the $\delta^{13}C$ of dissolved inorganic carbon in southern ocean deep water: Implications for glacial ocean circulation models, *Paleoceanography*, *8*, 587–610, doi:10.1029/93PA01291.

Mackensen, A., M. Rudolph, and G. Kuhn (2001), Late Pleistocene deep-water circulation in the subantarctic eastern Atlantic, *Global Planet. Change*, *30*, 197–229, doi:10.1016/S0921-8181(01)00102-3.

Marchitto, T. M., J. Lynch-Stieglitz, and S. R. Hemming (2005), Deep Pacific $CaCO_3$ compensation and glacial–interglacial atmospheric CO_2, *Earth Planet. Sci. Lett.*, *231*, 317–336.

Matsumoto, K., and J. Lynch-Stieglitz (1999), Similar glacial and Holocene deep water circulation inferred from southeast Pacific benthic foraminiferal carbon isotope composition, *Paleoceanography*, *14*(2), 149–163, doi:10.1029/1998PA900028.

Matsumoto, K., T. Oba, J. Lynch-Stieglitz, and H. Yamamoto (2002), Interior hydrography and circulation of the glacial Pacific Ocean, *Quat. Sci. Rev.*, *21*, 1693–1704.

McCave, I. N., L. Carter, and I. R. Hall (2008), Glacial–interglacial changes in water mass structure and flow in the SW Pacific Ocean, *Quat. Sci. Rev.*, *27*(19), 1886–1908.

McCorkle, D. C., P. A. Martin, D. W. Lea, and G. P. Klinkhammer (1995), Evidence of a dissolution effect on benthic foraminiferal shell chemistry: $\delta^{13}C$, Cd/Ca, Ba/Ca, and Sr/Ca results from the Ontong Java Plateau, *Paleoceanography*, *10*(4), 699–714, doi:10.1029/95PA01427.

Millo, C., M. Sarnthein, A. Voelker, and H. Erlenkeuser (2006), Variability of the Denmark Strait overflow during the last glacial maximum, *Boreas*, *35*(1), 50–60.

Ninnemann, U. S., and C. D. Charles (2002), Changes in the mode of Southern Ocean circulation over the last glacial cycle revealed by foraminiferal stable isotopic variability, *Earth Planet. Sci. Lett.*, *201*(2), 383–396.

Oliver, K. I. C., B. A. A. Hoogakker, S. Crowhurst, G. M. Henderson, R. E. M. Rickaby, N. R. Edwards, and H. Elderfield (2010), A synthesis of marine sediment core $\delta^{13}C$ data over the last 150 000 years, *Clim. Past*, *6*, 645–673, doi:10.5194/cp-6-645-2010.

Prentice, I. C., S. P. Harrison, and P. J. Bartlein (2011), Global vegetation and terrestrial carbon cycle changes after the last ice age, *New Phytol.*, *189*(4), doi:10.1111/j.1469-8137.2010.03620.x.

Runge, C. (1901), Über empirische Funktionen und die Interpolation zwischen äquidistanten Ordinaten, *Z. Math. Phys.*, *46*, 224–243.

Sabine, C. L., et al. (2004), The oceanic sink for anthropogenic CO_2, *Science*, *305*(5682), 367–371.

Schmittner, A., N. Gruber, A. C. Mix, R. M. Key, A. Tagliabue, and T. K. Westberry (2013), Biology and air–sea gas exchange controls on the distribution of carbon isotope ratios ($\delta^{13}C$) in the ocean, *Biogeosciences*, *10*, 5793–5816.

Shackleton, N. J. (1977), Carbon-13 in Uvigerina: Tropical rain forest history and the equatorial Pacific carbonate dissolution cycle, in *The Fate of Fossil Fuel in the Oceans*, edited by N. R. Andersen and A. Malahoff, pp. 401–427, Plenum, New York. [Available at http://www.esc.cam.ac.uk/research/research-groups/delphi.]

Siegenthaler, U., and J. L. Sarmiento (1993), Atmospheric carbon dioxide and the ocean, *Nature*, *365*(6442), 119–125.

Sigman, D. M., and E. A. Boyle (2000), Glacial/interglacial variations in atmospheric carbon dioxide, *Nature*, *407*, 859–869.

Smith, H. J., H. Fischer, M. Wahlen, D. Mastroianni, and B. Deck (1999), Dual modes of the carbon cycle since the Last Glacial Maximum, *Nature*, *400*, 248–250.

Spero, H. J., J. Bijma, D. W. Lea, and B. E. Bemis (1997), Effect of seawater carbonate concentration on foraminiferal carbon and oxygen isotopes, *Nature*, *390*(6659), 497–500.

Stern, J. V., and L. E. Lisiecki (2013), North Atlantic circulation and reservoir age changes over the past 41,000 years. *Geophys. Res. Lett.*, *40*, 3693–3697, doi:10.1002/grl.50679.

Tagliabue, A., L. Bopp, D. M. Roche, N. Bouttes, J. C. Dutay, R. Alkama, M. Kageyama, E. Michel, and D. Paillard (2009), Quantifying the roles of ocean circulation and biogeochemistry in governing ocean carbon-13 and atmospheric carbon dioxide at the last glacial maximum, *Clim. Past*, *5*(4), 695–706.

Woodruff, F., S. M. Savin, and R. G. Douglas (1980), 13C values of Miocene Pacific benthic foraminifera: Correlations with sea level and biological productivity, *Geology*, *13*, 119–122.

Zahn, R., K. Winn, and M. Sarnthein (1986), Benthic foraminiferal $d^{13}C$ and accumulation rates of organic carbon: Uvigerina peregrina group and Cibicidoides wuellerstorfi, *Paleoceanography*, *1*(1), 27–42, doi:10.1029/PA001i001p00027.

Zhang, J., P. D. Quay, and D. O. Wilbur (1995), Carbon isotope fractionation during gas-water exchange and dissolution of CO_2, *Geochim. Cosmochim. Acta*, *59*(1), 107–114.